# First investigations on controlling unbalanced flexible rotors using shaft seals

Thomas KLETSCHKOWSKI[1]

[1] Hamburg University of Applied Sciences, Germany

## ABSTRACT

To analyze the vibration behavior of an unbalanced flexible rotor considering both internal damping and a constant driving torque, the Laval-rotor-model is applied. The resulting set of nonlinear ordinary differential equations is transformed into a dimensionless formulation to enable numerical integration using an explicit Runge-Kutta-schema. Applying this approach it is possible to study two different phenomena, the well known “stalling” effect of the shaft that occurs just below the bending critical speed when the drive torque is too weak to pass the resonance as well as the effect of self-excitation that occur at very high speeds because of negative damping. It is shown that both problems can be solved, if the radial displacements of the shaft are controlled by a shaft seal. The latter is modeled as a lumped system – considering mass, stiffness and viscosity effects. The seal influences both the horizontal and vertical displacement of the shaft, and the speed of rotation. Because shaft seals are already used as sensors to determine the speed of rotation, it should be possible to develop a control approach to adjust the pressure between seal and shaft in such a way that stalling and self-excitation can be avoided or at least reduced.

Keywords: Flexible rotor, shaft seal I-INCE Classification of Subjects Number: 44

## 1. INTRODUCTION

The reduction of mechanical vibrations as well as the reduction of air-borne noise and structure-borne noise is not only essential to ensure safe operational conditions. It is also necessary to ensure the acceptance noise generated by machineries of different kind. A typical example is a wind power station (WPS) that can only be realized, if the impact on both nature and living environment is accepted by the society.

As for automotive and airplane engines, the dynamic behavior of rotating machinery parts in a WPS has to be controlled to avoid unwanted or critical vibrations. Special problem connected with rotor dynamics occur, if the rotor has to pass “critical speeds” or if internal damping has to be taken into account as shown in Reference (1, 2). To avoid “stalling” at a resonance frequency, the driving torque must be sufficient to accelerate the rotor through the critical speed. In order to avoid instabilities caused by internal damping, it is necessary to realize a proper amount of external damping, as shown in Reference (3), – in a best case scenario without significant reduction of the driving torque.

In the present paper, the bending vibration behavior of an unbalanced flexible rotor considering both internal damping and a constant driving torque is analyzed using the Laval-rotor-model, compare Reference (1, 2). In order to evaluate the potential of rotary shaft seals that could be used to control the radial deflections, the seal is modeled as a lumped system – considering mass, stiffness and viscosity effects. This approach is based of the findings presented in Reference (4). It has recently also been applied to perform first investigations on actuation forces in adaptive rotary shaft seals, see Reference (5).

The present paper is structured as follows. A simplified mechanical model of the dynamical system (internally damped, unbalanced, flexible rotor with rotary shaft seal) and the resulting differential equations are described in section 2. The results of numerical investigations (without and with shaft seal) are discussed in section 3. Main results are summarized in section 4. This last section also includes an outlook on future steps.

[1] Thomas.kletschkowski@haw-hamburg.de

## 2. A SIMPLE MODEL OF FLEXIBLE ROTOR WITH SHAFT SEAL

To derive a simplified mechanical model, the Laval-rotor-model, see (1, 2), is used to describe the unbalanced flexible rotor. As illustrated by Figure 1 (left) the dynamic mass ($m$), compare Reference (3), is concentrated in a plane disk (without inclination). The disk is placed in the middle of the elastic shaft. As also shown in Reference (3), its bending stiffness ($EI$) can be converted to a stiffness parameter of an elastic spring. The bearings are rigid and allow for rotation.

As shown in Reference (4) and applied in Reference (5), the rotary shaft seal can be modeled as a lumped system too. As illustrated by figure 1 (right) it is necessary to consider the mass of the sealing edge ($m_s$), the compressibility of the sealing edge ($k_{sh}$), the bending stiffness of the seal ($k_s$) as well as damping effects ($b_s$). Because dry friction between seal and shaft is in practice significantly reduced by a lubricating oil film, the contact between seal and shaft is modeled as normal contact without friction in circumferential direction. Furthermore perfect followability is assumed (no separation between seal and shaft). In order to analyze the effect of the shaft seal on the radial deflection of the shaft, it is assumed that the seal is also mounted in the vicinity of the disk.

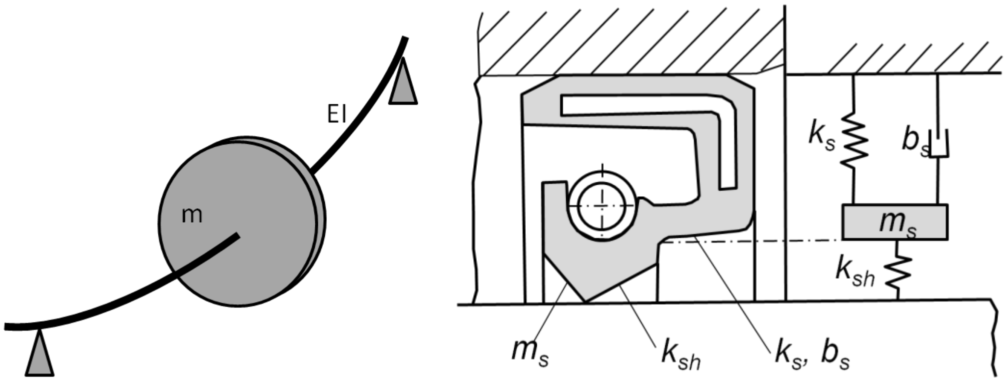


Figure 1 – Mechanical modeling of elastic rotor with seal, compare also (5), (7)

Before the equations of motion can be discussed, it is necessary to recall important kinematic equations. The deflection of the rotating shaft is caused by unbalanced forces acting in the center of gravity ***s***, compare Figure 2. All other forces are acting directly on the shaft. The deflection of the shaft is measured at the midpoint of the disk ***w***. The distance between these points is given by the eccentricity $\varepsilon$. Their rotation around the connection line between the bearings is described by $\varphi$. As illustrated by Figure 2, the relation between the horizontal/vertical displacement of the center of gravity and the horizontal/vertical displacement of the disk position at the shaft is given by

$$y_s = y_w + \varepsilon \sin(\varphi) \tag{1}$$

$$z_s = z_w + \varepsilon \cos(\varphi) . \tag{2}$$

Because all coordinates are time-dependent, the relation for the associated velocities reads

$$\dot{y}_s = \dot{y}_w + \varepsilon \cos(\varphi)\dot{\varphi} \tag{3}$$

$$\dot{z}_s = \dot{z}_w - \varepsilon \sin(\varphi)\dot{\varphi} . \tag{4}$$

Finally the relation between the associated accelerations is given by

$$\ddot{y}_s = \ddot{y}_w - \varepsilon \sin(\varphi)\dot{\varphi}^2 + \varepsilon \cos(\varphi)\ddot{\varphi} \tag{5}$$

$$\ddot{z}_s = \ddot{z}_w - \varepsilon \cos(\varphi)\dot{\varphi}^2 - \varepsilon \sin(\varphi)\ddot{\varphi} . \tag{6}$$

If, and only if, the rotor runs with a constant speed ($\Omega \equiv \dot{\varphi} = \text{const.}$), Equation (1) and (2) can be replaced by the well known relations

$$y_s = y_w + \varepsilon \sin(\Omega t + \varphi_0) \tag{7}$$

$$z_s = z_w + \varepsilon \cos(\Omega t + \varphi_0) , \tag{8}$$

where $\varphi_0$ represents an initial condition.

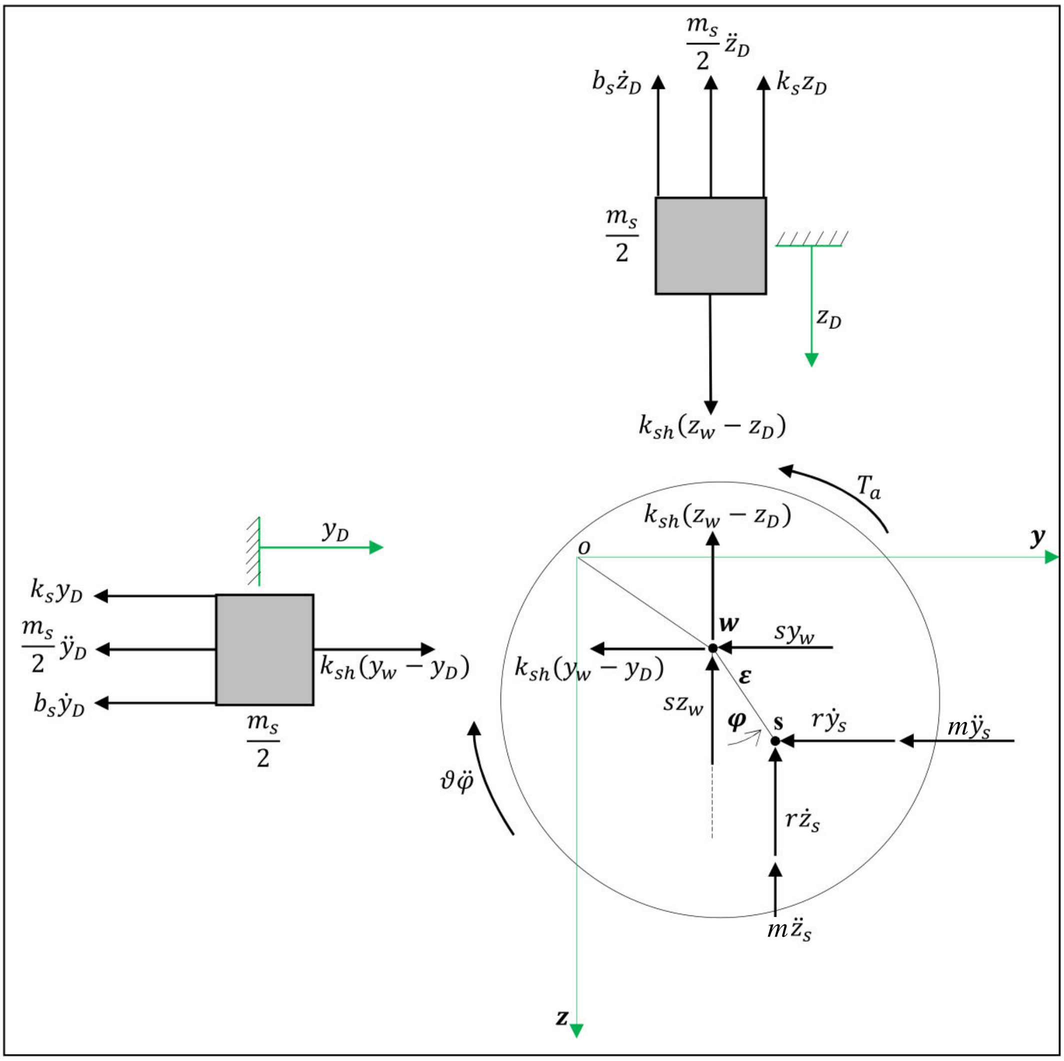


Figure 2 – Free-body-diagram (FBD) for the seal-shaft-problem (SSP), compare (6)

Figure 2 contains the free-body-diagram (FBD) for the seal-shaft-problem (SSP). It can be seen that the dynamic mass of the seal $m_s$ is split into two parts, both representing 50% of the seal body. The coordinates for the horizontal/vertical displacement of the seal are indicated by the subscript *D*. Furthermore the directions of the driving torque $T_a$ and the direction of mass moment of inertia $\vartheta\ddot{\varphi}$ are shown. The equivalent stiffness of the shaft is represented by *s*. For simplicity, the forces resulting from internal damping are not shown in Figure 2. For this reason, the equations of motion, according to the FBD are

$$m\ddot{y}_s + r\dot{y}_s + (s + k_{sh})\, y_s = k_{sh} y_D + \varepsilon (s + k_{sh}) \sin(\varphi) \tag{9}$$

$$\frac{m_s}{2}\ddot{y}_D + b_s \dot{y}_D + (k_s + k_{sh})\, z_s = k_{sh} y_s - k_{sh}\varepsilon \sin(\varphi) \tag{10}$$

$$m\ddot{z}_s + r\dot{z}_s + (s + k_{sh})\, z_s = k_{sh} z_D + \varepsilon (s + k_{sh}) \cos(\varphi) \tag{11}$$

$$\frac{m_s}{2}\ddot{z}_D + b_s \dot{z}_D + (k_s + k_{sh})\, z_D = k_{sh} z_s - k_{sh}\varepsilon \cos(\varphi) \tag{12}$$

$$\vartheta\ddot{\varphi} = T_a + \varepsilon\left[(s + k_{sh})\cos(\varphi)\, y_s - (s + k_{sh})\sin(\varphi)\, z_s - k_{sh}\cos(\varphi)\, y_D + k_{sh}\cos(\varphi)\, z_D\right] \text{ with } \vartheta = mk^2\,, \tag{13}$$

where $k$ is the radius of inertia.

Internal damping is considered by forces acting on the shaft at the position of the disk. The derivation of these forces is shown in Reference (2, 3). According to these references, the forces specified in Equation (14) have been added to Equation (9). The forces specified in Equation (15) have been added to Equation (10).

$$F_y^i = -b_i\dot{\varphi} z_w + b_i\dot{y}_w = b_i\dot{y}_s - 2b_i\varepsilon\dot{\varphi}\cos(\varphi) + b_i\dot{\varphi} z_s \tag{14}$$

$$F_z^i = +b_i\dot{\varphi} y_w + b_i\dot{z}_w = b_i\dot{z}_s + 2b_i\varepsilon\dot{\varphi}\sin(\varphi) - b_i\dot{\varphi} y_s \tag{15}$$

To complete Equation (13), the torques specified in Equation (16) have been considered.

$$M_x^i = \varepsilon\cos(\varphi)F_y^i - \varepsilon\sin(\varphi)F_z^i \tag{16}$$

To prepare a numerical evaluation of the equations of motion a dimensionless (short dimless) approach has been used. Such an approach, compare Reference (3), starts with the definition of the dimensionless time $t \mapsto \tau := \omega t$, where $\omega := \sqrt{s/m}$ is known as the natural frequency of the undamped system without shaft seal. After introduction of the dimensionless time, it is possible to replace any time derivative such as

$$\dot{x} := \frac{dx}{dt} = \frac{dx}{d\tau}\frac{d\tau}{dt} = \omega\frac{dx}{d\tau} := \omega x' \text{ and } \ddot{x} := \frac{d\dot{x}}{dt} = \frac{d\dot{x}}{d\tau}\frac{d\tau}{dt} = \omega^2\frac{dx}{d\tau} := \omega^2 x''. \tag{17}$$

Furthermore any displacement can be normalized by the eccentricity such as

$$Y_s := y_s/\varepsilon,\quad Z_s = z_s/\varepsilon,\quad Y_D = y_D/\varepsilon,\quad Z_D = z_D/\varepsilon \tag{18}$$

If Equation's (9) – (12) are normalized by the dynamic mass of the rotor $m$, and if in addition Equation (13) is normalized by $\vartheta$, the dimensionless equations of motion are

$$Y_s'' + 2DY_s' + (1+\nu)Y_s = \nu Y_D + (1+\nu)\sin(\varphi) \tag{19}$$

$$\frac{\alpha}{2}Y_D'' + 2D\beta Y_D' + \nu\left(1+\nu_1^{-1}\right)Y_D = \nu Y_s - \nu\sin(\varphi) \tag{20}$$

$$Z_s'' + 2DZ_s'' + (1+\nu)Z_s = \nu Z_D + (1+\nu)\cos(\varphi) \tag{21}$$

$$\frac{\alpha}{2}Z_D'' + 2D\beta Z_D' + \nu\left(1+\nu_1^{-1}\right)Z_D = \nu Z_s - \nu\cos(\varphi) \tag{22}$$

$$\varphi'' = T + e\left[(1+\nu)\cos(\varphi)Y_s - (1+\nu)\sin(\varphi)Z_s - \nu\cos(\varphi)Y_D + \nu\sin(\varphi)Z_D\right], \tag{23}$$

where the following abbreviations have been used:

- External damping ratio for rotor: $D := r/\sqrt{4ms}$
- Stiffness ratio seal-shaft: $\nu := k_{sh}/s$
- Stiffness ration seal-seal: $\nu_1 := k_{sh}/k_s$
- Mass ratio seal-shaft: $\alpha := m_s/(2m)$
- Damping ratio seal-shaft: $\beta := b_s/r$
- Dimensionless driving torque: $T := T_a/\left(\vartheta\omega^2\right)$
- Dimensionless squared eccentricity: $e := \varepsilon^2/k^2$ .

The dimensionless formulations of Equation (14), (15) and (16) are

$$\frac{F_y^i}{m\varepsilon\omega^2} = 2D\beta_i\left[Y_s' - \left(2\cos(\varphi) - Z_s\right)\varphi'\right] \tag{24}$$

$$\frac{F_z^i}{m\varepsilon\omega^2} = 2D\beta_i\left[Z_s' + \left(2\sin(\varphi) - Y_s\right)\varphi'\right] \tag{25}$$

$$\frac{M_x^i}{\vartheta\omega^2} = 2D\beta_i e\left[Y_s'\cos(\varphi) - Z_s'\sin(\varphi) + \left(Z_s\cos(\varphi) + Y_s\sin(\varphi) - 2\right)\varphi'\right], \tag{26}$$

where $\beta_i := b_i/r$ is the internal damping ratio for rotor.

# 3. NUMERICAL INVESTIGATIONS

## 3.1 Flexible Rotor without seal

The model specified by Equation (19)-(23) has been used for numerical simulation of the transient dynamic behavior of the unbalanced flexible rotor without seal. The model equations have been transformed into a system of first order differential equations. This system has been solved using a fourth-order explicit Runge-Kutta-schema with constant time-stepping. Following the procedure described in Reference (1), all initial conditions have been set to zero, except for the vertical displacement of the shaft. The latter has been described by a unit deflection of magnitude "1". This set of initial conditions describes the start-up of an undeflected shaft from a stand-still position. The eccentricity at the time $\tau = 0$ lies in $z$-direction. The parameter set listed in Table 1, compare Reference (2), has been used to simulate the stalling effect.

Table 1 – Simulation of flexible rotor without seal (stalling effect)

| $D$ | $\beta_i$ | $e$ | $T$ |
|---|---|---|---|
| 0,020 | 0,0 | 0,001 | 0,010 |

In order to simulate the effect self-excitation caused by internal damping, the driving torque must be strong enough to accelerate the shaft through the critical speed. For this reason the driving torque has been slightly increased, compare Table 2. Furthermore it has been assumed that the amount of internal damping matches the amount of external damping.

Table 2 – Simulation of flexible rotor without seal (instability effect)

| $D$ | $\beta_i$ | $e$ | $T$ |
|---|---|---|---|
| 0,020 | 1,0 | 0,001 | 0,012 |

The associated simulation results are shown in Figure 3 and Figure 4, respectively. In both figures the vertical displacement of the shaft $z_w$ normalized to its maximum value $z_w^{\max}$ is shown using a blue curve. Furthermore the rotating speed $\varphi'$ is shown using a red colored curve.

The results shown in Figure 3 clarify that an insufficient driving torque is not able to accelerate the rotor through its first critical speed. The rotor stalls at its natural frequency. Below the critical speed, the rotating speed increases linearly with time – the shaft rotates with constant acceleration. This changes, if the rotor stalls in its first critical speed. In this situation the shaft rotates (under nearly stationary conditions) with a rotating speed that varies around a constant mean.

The results shown in Figure 4 prove that the rotor is able to pass the critical speed, if the driving torque is sufficient high. After passing the natural frequency, the rotating speed is again constant in time and the shaft is accelerated by the driving torque. But, at very high speeds, the homogenous solution becomes unstable because of positive real parts in the eigenvalues, compare Reference (3).

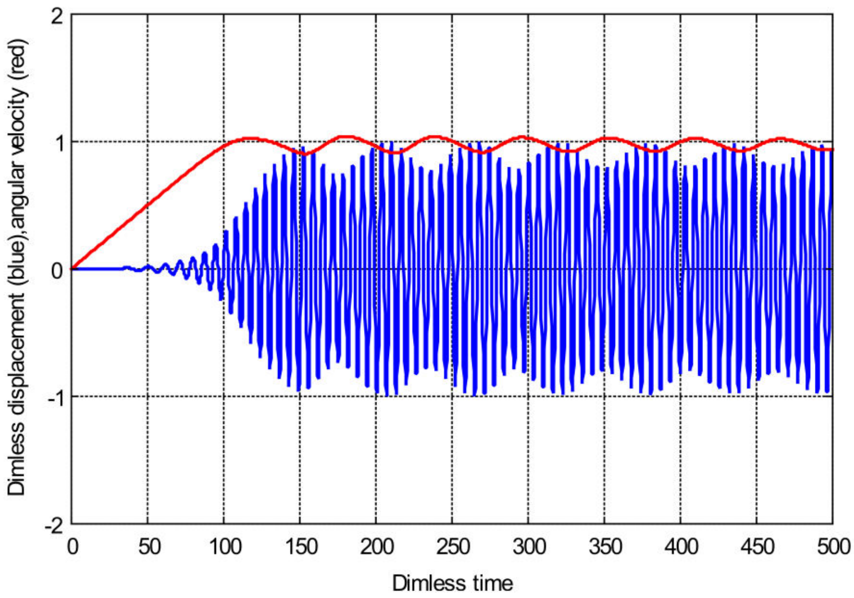


Figure 3 – Flexible rotor (without seal) stalling at critical speed

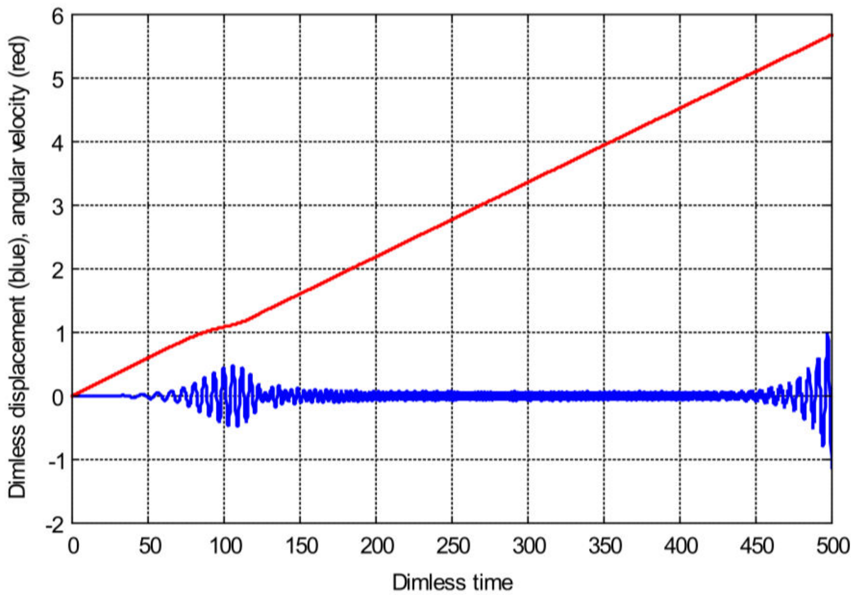


Figure 4 – Unstable run of flexible rotor (without seal) at very high speeds

### 3.2 Flexible Rotor with seal

To avoid both stalling at the critical speed and instability due to internal damping, the effect of a shaft seal has been taking into account. Now the model specified by Equation (19)-(26) has been used for numerical simulation of the transient dynamic behavior of the unbalanced flexible rotor with seal.

The parameter listed in Table 3 and in Table 4 has been used in these simulations. It can be seen that only 1.5% of the dynamic mass of the rotor are required to model the dynamic mass of the seal. Furthermore the compressibility of the sealing edge equals only 7% of the shaft bending stiffness. It can also be seen that the compressibility of the sealing edge is nine time higher as the bending stiffness of the seal. In all simulations the external damping caused by the shaft seal nearly equals the amount of external damping. The choice of this parameter set proves that a highly flexible seal with low viscosity as well as low dynamic mass (compared to the rotating shaft) has been taken into account in the numerical investigations.

Table 3 – Simulation of flexible rotor with seal (no stalling effect)

| $D$ | $\beta_i$ | $\beta$ | $\alpha$ | $\nu$ | $\nu_1$ | $e$ | $T$ |
|---|---|---|---|---|---|---|---|
| 0,020 | 1,0 | 1,076 | 0,0075 | 0,07 | 9,0 | 0,001 | 0,010 |

Table 4 – Simulation of flexible rotor with seal (no instability effect)

| $D$ | $\beta_i$ | $\beta$ | $\alpha$ | $\nu$ | $\nu_1$ | $e$ | $T$ |
|---|---|---|---|---|---|---|---|
| 0,020 | 1,0 | 1,076 | 0,0075 | 0,07 | 9,0 | 0,001 | 0,012 |

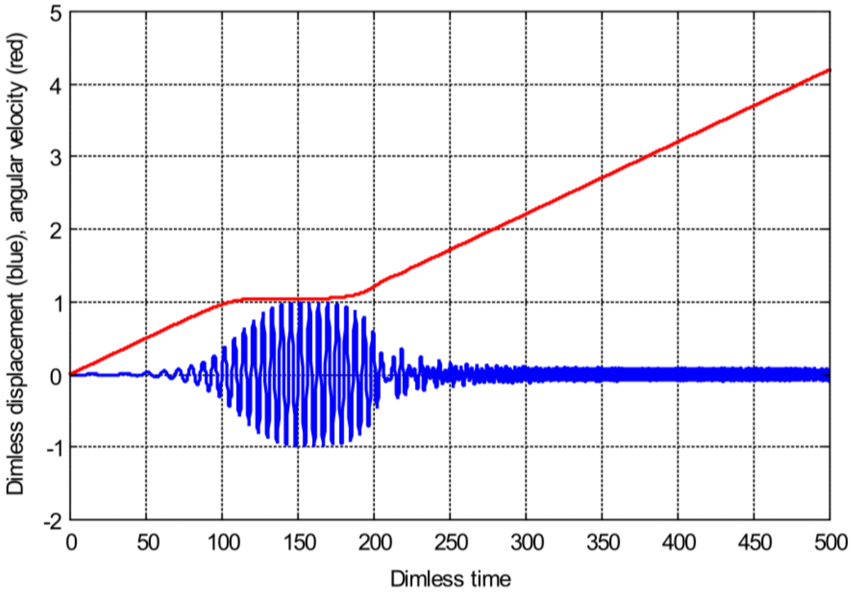


Figure 5 – Flexible rotor with seal, not stalling at critical speed

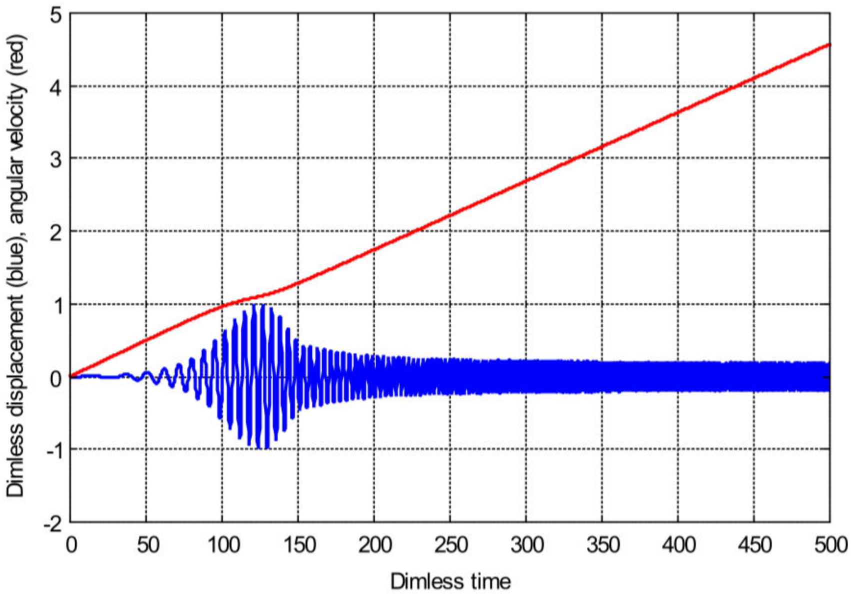


Figure 6 – Stable run of flexible rotor with seal at very high speeds

The numerical results shown in Figure 5 and Figure 6 prove that a (proper chosen) rotary shaft seal is capable to avoid the effect of stalling at the critical speed as well as to suppress instabilities caused by internal damping.

The results shown in Figure 5 are associated to the lower driving torque. For this reason, the shaft is in danger to stall at the natural frequency of the shaft. Because of the interaction between seal and shaft it is possible to reduce the deflection of the shaft. This seems to be feasible, because the soft sealing element is compress in horizontal and vertical direction and therefore able to dissipate energy. However, it is necessary to point out that a feedback on the driving torque caused by an additional friction moment that results from the pressure between seal and shaft has not been taken into account.

The results shown in Figure 6 prove that a small increase in external damping is capable to avoid instabilities. This is a very interesting result, because the (temporal and/or adaptive) increase of the radial pressure between seal and shaft could be one method to realize the stability improvement of motion of a rotor with an active control method, as discussed in Reference (8).

## 4. CONCLUSIONS

The numerical investigations presented in this paper indicate that rotary shaft seals can be capable to control mechanical vibrations of rotating machineries. But, from a critical point of view it must be noticed that the feasibility has been demonstrated using simplified mechanical models only – such as the Laval-rotor-model. Furthermore, dry and/or fluid friction between seal and shaft has not been taken into account. The same holds for the radial stiffness and viscosity of the oil film between seal and shaft as well as for thermo-mechanical coupling effects. All effects have been studied using a limited set of system parameters. An optimization procedure, applied to find the best suited system parameters is not yet performed. And also actuation principles such as shape memory effects, required for some adjustment of sealing performance, have not been taken into account. Some of these problems are subjected to an ongoing PhD-theses, see Reference (9), and therefore part of future research.

## ACKNOWLEDGEMENTS

The author gratefully acknowledges the support of Mr. Kean Hong Chew and Mr. El Ayachi Lahrach for the support of this publication, especially for their permission to use Figure 2 in the present paper. The author also acknowledges the support of the Urban Mobility Lab team at the University of Applied Sciences Hamburg for providing an inspiring frame for applied research.

## REFERENCES

1. Gasch R, Markert R, Pfützner H. Acceleration of unbalanced flexible rotors through the critical speeds. J Sound and Vibration. 1978;63(3):393-409.
2. Gasch R, Nordmann R, Pfützner H. Rotordynamik. Berlin and Darmstadt, Germany: Springer; 2005.
3. Brommundt E, Sachau D. Schwingungslehre mit Maschinendynamik. Wiesbaden, Germany: Teubner; 2008.
4. Neumann K-H. Ein Beitrag zur Dichtwirkung von Radialwellendichringen unter besonderer Berücksichtigung dynamischer Beanspruchungen. Dissertation, Ingenieurhochschule Zwickau, Zwickau, Germany: 1983.
5. Kletschkowski T, Malcherczyk P. First investigations on actuation forces in adaptive rotary shaft seals. Proc 18th ISC International Sealing Conference, 8-9 October 2014, Stuttgart, Germany 2014.
6. Chew K-H, Lahrach El Ayachi. Numerische Untersuchungen zur Interaktion eines elastischen Rotors mit einem Radialwellendichtring. Masterprojekt, HAW Hamburg, supervised by Prof. Dr.-Ing. habil. Kletschkowski, Hamburg, Germany 2014.
7. Kletschkowski T. Theoretische Untersuchungen zur Beruhigung der Resonanzdurchfahrt mit Wellendichtringen. In: K.-F. Berger/S. Kiefer (Hrsg.) DICHTUNGSTECHNIK JAHRBUCH 2016, Germany: Hüthing; 2015. p .252-259.
8. Liao M, Gasch R, Kolk O, Kletschkowski T. Stability improvement of motion of a rotor with an active control method. J. of Vibration and Control. 2000; 6:291-308.
9. Schnelle thermo-mechanische Simulation der Dynamik von Radialwellendichtungen, PhD-thesis, carried out at the University of Applied Sciences Hamburg, supervised by Prof. Dr.-Ing. habil. Kletschkowski, Hamburg, Germany 2016.